J. Cell Sci. 83, 251–267 (1986)
Printed in Great Britain © The Company of Biologists Limited 1986

KINETIC PROPERTIES OF MICROTUBULE-ACTIVATED 13 S AND 21 S DYNEIN ATPases

EVIDENCE FOR ALLOSTERIC BEHAVIOUR ASSOCIATED WITH THE INNER ROW AND OUTER ROW DYNEIN ARMS

FRED D. WARNER AND JANE H. McILVAIN

Department of Biology, Biological Research Laboratories, Syracuse University, Syracuse, NY 13210, USA

SUMMARY

The 13 S and 21 S dynein ATPases from *Tetrahymena* cilia rebind to extracted doublet microtubules as inner row and outer row arms. Rebinding is accompanied by four- to ninefold activation of the ATPase activity. The soluble (microtubule-free) forms of the two dyneins exhibit simple saturation kinetics ($h = 1{\cdot}0$) with $V_{max} \ll 1$ μmol $P_i\,mg^{-1}\,min^{-1}$ and $K_m = 20$–40 μM-ATP. Mixing a fixed quantity of free dynein with increasing concentrations of extracted doublets results in systematic increases in all three kinetic parameters for each dynein. At infinite concentrations of doublets and ATP, each enzyme undergoes a significant shift to sigmoid saturation kinetics ($h = 2$–3), V_{max} increases to a turnover rate of about 90 mol ATP per mol $E\,s^{-1}$ and the Michaelis constant increases to $\geqslant 100$ μM-ATP. These data suggest that both enzymes are allosteric and can be interpreted in terms of positive cooperativity relative to a minimum of two or three interacting sites. It is less clear whether this cooperativity is related to subunit interactions within the 21 S or 13 S particles, or to subunit interactions between adjacent particles (arms) on the microtubule lattice.

INTRODUCTION

The dynein ATPases from cilia or flagella occur in two forms that are distinguishable by their physicochemical properties as well as by their structure and organization. In native *Tetrahymena* cilia, 21 S dynein or dynein 1 occupies the outer row arm position while 13 S dynein or dynein 2 occupies the inner row arm position (Warner *et al.* 1985). The 21 S particle is structurally complex (Goodenough & Heuser, 1984), comprising three different high molecular weight ATPases ($M_r \cong 400\,000$) and numerous other polypeptides of unknown function (Porter & Johnson, 1983). Each of the three high molecular weight subunits has a binding site for microtubules and an active site recognizing $MgATP^{2-}$ (Johnson, 1983). The ATPase activity of both 13 S and 21 S dyneins is activated by microtubules (Warner *et al.* 1985), while substrate binding by 21 S dynein dissociates the resulting tubulin–dynein complex (Mitchell & Warner, 1981; Johnson, 1983).

Rebinding of 21 S dynein to extracted doublet microtubules exhibits sigmoid behaviour (Warner & McIlvain, 1982), although it is unlikely that this behaviour represents true cooperative interactions between tubulin-binding domains of the

Key words: cilia, 13 S and 21 S dynein ATPases, saturation kinetics, positive cooperativity.

dynein particle. Instead, it is probably related to weak interactions between adjacent dynein particles as they reassociate with the microtubule lattice. Goodenough & Heuser (1984) have shown that the structure usually identified as an outer row dynein arm is a composite image constructed from two overlapping 21 S particles. This finding implies the existence of specific interactions between subunits of adjacent dynein arms. The structure and organization of 13 S dynein has not been thoroughly characterized, although recent data indicate that, while the particles may not overlap, they do exhibit considerable structural complexity and probably comprise two high molecular weight ATPases (Piperno & Luck, 1981; Porter & Johnson, 1983) that are related in overall organization to the radial spokes (Goodenough & Heuser, 1985; Warner *et al.* 1985).

The elaborate structure of the 13 S and 21 S dynein particles implies the existence of interactions between subunit domains that would probably be expressed as positive or negative cooperativity relative to substrate saturation kinetics. However, the soluble or microtubule-free conformations of the dyneins have usually exhibited simple saturation kinetics (no cooperativity). We recently demonstrated the capacity to rebind differentially the isolated 13 S and 21 S dyneins from *Tetrahymena* cilia to the inner row and outer row arm positions. Rebinding activates the ATPase activity of each dynein. By using differential rebinding of the two ATPases, we are now able to characterize the kinetic properties of each enzyme independently and also describe the mechanism of activation induced by microtubules with respect to cooperativity, enzyme velocity and substrate affinity.

MATERIALS AND METHODS

Dynein and microtubule preparations

Cilia were isolated from cultures of *Tetrahymena thermophila*, mucocyst-free strain B-255, by methods described elsewhere (Mitchell & Warner, 1980). All isolation, extraction and resuspension solutions contained 0·1 mM-EGTA and 0·01 mM-leupeptin.

Cilia were demembranated by one exposure to 0·1 % Nonidet P40, collected by centrifugation, and resuspended in 20 mM-HEPES, 0·1 mM-EGTA (pH 7·4). In order to prepare twice-extracted doublets, dynein extraction was done in 0·5 M-KCl, 10 μM-ATP, 10 μM-vanadate for 25 min, followed by desalting of the subsequent pellet fraction and low ionic strength dialysis against 1 mM-HEPES, 0·1 mM-EGTA, for 24 h. Twice-extracted doublets were collected by centrifugation and resuspended in 6 mM-$MgCl_2$, 20 mM-HEPES, 0·1 mM-EGTA (pH 7·4). The dynein-containing supernatant fraction from the KCl/ATP extraction was dialysed against 10 mM-HEPES, 0·1 mM-EGTA and concentrated to 0·5–1 mg ml^{-1} on an Amicon PM30 membrane. The concentrated extract was fractionated on calibrated linear 0 to 30 % sucrose density gradients (Mitchell & Warner, 1981). ATPase-containing fractions from the gradient were redialysed against 10 mM-HEPES, 0·1 mM-EGTA and reconcentrated to 1–2 mg ml^{-1} on the Amicon membrane.

Dynein ATPase assays

All dynein ATPase assays were done at 20 °C in a standard assay buffer containing 6 mM-$MgCl_2$, 0·1 mM-EDTA, 40 mM-HEPES, 1 mM-ATP (pH 7·4). For kinetic experiments, $MgCl_2$ was added 5 mM in excess of the ATP concentration. The reaction was initiated by addition of ATP and terminated by addition of cold trichloroacetic acid (TCA). The inorganic phosphate released was measured ($A_{660\,nm}$) by the method of Taussky & Shorr (1953). Specific activity was calculated from triplicate determinations for the linear region of phosphate release (5 min) at both subsaturating

and saturating ATP concentrations. Enzyme concentrations used in the assays were 8 $\mu g\,ml^{-1}$ for both the 13 S and 21 S dyneins.

For kinetic experiments or experiments using subsaturating concentrations of ATP, a stable ATP concentration was maintained by using an ATP-regenerating system consisting of 2 mM-phosphoenol pyruvate and pyruvate kinase (23 $\mu g\,ml^{-1}$) added to the standard assay buffer (Mitchell & Warner, 1980). Kinetic data were expressed as μmoles of inorganic phosphate (P_i) released per mg of enzyme or protein per minute. The data were analysed and kinetic constants derived by using the non-linear least squares computer program described previously (Warner & McIlvain, 1982; Warner *et al.* 1985).

Protein concentrations for all procedures were determined by the Coomassie Blue dye binding technique (Bradford, 1976) as modified by Read & Northcote (1981), using bovine serum albumin (BSA) as a protein standard. For experiments involving variable concentrations of a given protein, the concentration sequence was derived by serial dilution of a known concentration.

RESULTS

A description of the kinetic analysis

All kinetic data were analysed by an unweighted, non-linear least squares curve-fitting computer program derived from the Hill equation. Two equations were used, equation (1) for simple hyperbolic kinetics and equation (2) for more complex sigmoid kinetics. The program estimates by successive iteration the parameters of maximum velocity (V_{max}), Michaelis constant (K_m or $[S]_{0.5}$) and the Hill coefficient (h). The iterative process ceases when the relative change in the sum of squares is $<10^{-5}$.

$$V = \frac{V_{max}}{1 + \frac{K_m}{[S]}} \tag{1}$$

$$V = \frac{V_{max}}{1 + \left(\frac{K_m}{[S]}\right)^h} \tag{2}$$

The Hill coefficient is a measure of a curve fit to a rectangular hyperbola. When $h = 1{\cdot}0$, the data fit a hyperbola and exhibit simple saturation kinetics (no cooperativity). When h is $\geqslant 1{\cdot}0$, the data exhibit sigmoid kinetics consistent with positive cooperativity between subunits of the enzyme or its oligomer. When h is $\leqslant 1{\cdot}0$, the data exhibit anti-sigmoid kinetics, which, although consistent with negative cooperativity, are more likely to be related to a lack of homogeneity relative to the active sites in the enzyme preparation. The significance of values for h different from 1·0 was determined by an analysis of variance of the residual sum of squares resulting from use of the two non-linear equations (Warner & McIlvain, 1982).

For graphical illustration, kinetic data are expressed in direct plots (V *versus* [S]) as well as in Eadie–Scatchard plots ($V/[S]$ *versus* V) or Lineweaver–Burke plots ($1/V$ *versus* $1/[S]$), both of which linearize the relationship between the independent [S] and dependent (V) variables when $h = 1{\cdot}0$. However, all kinetic constants and

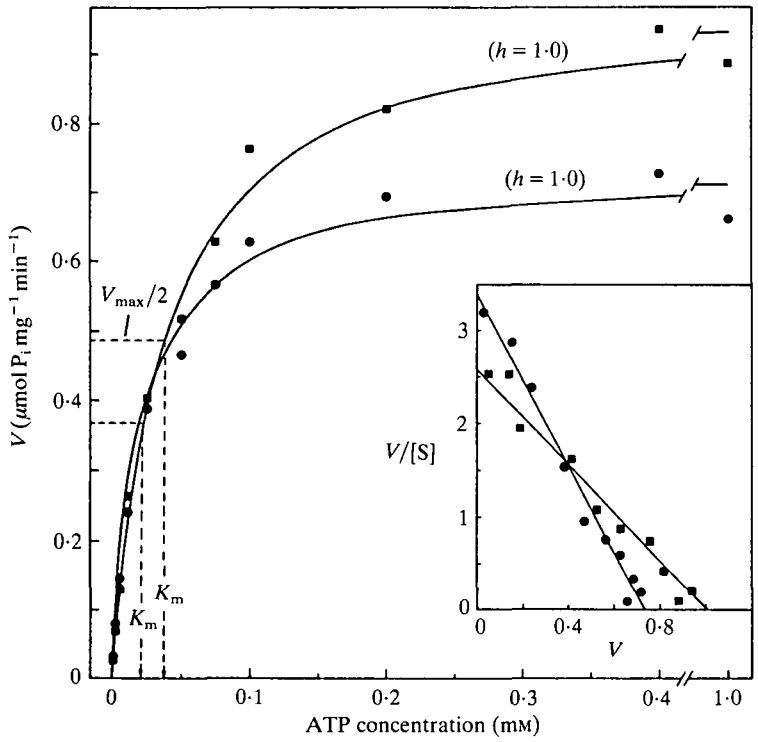

Fig. 1. Substrate (ATP) saturation kinetics (direct plot) for the soluble forms of the 13 S (■) and 21 S (●) dynein ATPases as fitted to the estimated dependent variables derived by eqn (1). Both enzymes exhibit simple saturation kinetics ($h = 1{\cdot}0$). The insert is an Eadie–Scatchard plot of the same data. The estimated kinetic parameters derived from these data are summarized in Table 1. $n = 10$ preparations of cilia.

estimated dependent variables were determined by equations (1) and (2) and were used to fit the curves in each of the three kinds of plots.

Kinetic properties of the microtubule-free dyneins

Substrate saturation kinetics (*V versus* [S]) for the soluble or microtubule-free forms of the 13 S and 21 S dyneins were analysed over an ATP concentration range of 1 μM to 1 mM at an enzyme concentration of 8 μg ml^{-1}. Ten individual preparations of cilia were examined, the resulting velocity data (μmol Pi mg^{-1} min^{-1}) were averaged and then analysed by equations (1) and (2). Both the 13 S and 21 S dyneins exhibit simple saturation kinetics (Fig. 1; $h = 1{\cdot}0$). None of the preparations examined showed significant deviation from hyperbolic kinetics and, therefore, the observed dependent variables (V) were best fitted by equation (1), since it has the fewest (two) estimated parameters.

The kinetic data for the soluble 13 S and 21 S dyneins are summarized in Table 1. Enzyme velocity at an infinite substrate concentration (V_{max}) was $\ll 1$ μmol P_i mg^{-1} min^{-1} for both enzymes, although 13 S dynein exhibited a considerably greater range of activity between preparations of cilia. The Michaelis constant (K_m) for 21 S dynein (21 μM-ATP) was about twofold lower than the K_m for 13 S dynein

(37 μM-ATP) but, again, 13 S dynein exhibited a considerably greater range of values that overlapped with the mean value for 21 S dynein. It should be noted that K_m was determined for total added ATP, not free $MgATP^{2-}$, and thus the reported values are slight overestimates ($\cong$17 %) of the true parameter.

We also examined the kinetic behaviour of twice-extracted (2×) doublets because, as will be seen, they represent an apparently activated, albeit residual activity enzyme preparation. Estimated parameters for the 2× doublets are also summarized in Table 1. The doublets exhibit anti-sigmoid kinetics ($h = 0{\cdot}8$) and have a considerably greater K_m (>100 μM-ATP) than the soluble dyneins, consistent with an activated enzyme preparation (see following sections). Although the mean value for h was <1·0, the parameter also had a broad range of frequently significant values both less than and greater than unity.

Before assessing the effects of extracted doublets on dynein ATPase activity, we first had to determine if any of the three enzyme preparations retained an endogenous substrate for the dyneins, or if the two dyneins retained an activator or inhibitor of ATPase activity. An endogenous substrate will result in a non-linear plot of velocity (μmol $P_i\,min^{-1}$) *versus* protein concentration when [S] is $<K_m$ and linear plots when [S] is $>K_m$. An endogenous activator that increases V_{max} or an inhibitor that decreases V_{max} will also result in non-linear plots of velocity *versus* [protein] but when [S] is either less than or greater than K_m.

The specific activity of extracted doublet microtubules (μmol $P_i\,mg^{-1}\,min^{-1}$) was determined for serially diluted protein concentrations of 0·02–0·51 mg ml^{-1} relative to 50 μM and 1 mM-ATP. The results obtained from three preparations of cilia are illustrated in Fig. 2. At protein concentrations <0·3 mg ml^{-1}, extracted doublets exhibit a strict linear relationship (constant specific activity) between velocity and concentration at both saturating and subsaturating concentrations of ATP (only data from saturating [ATP] are illustrated). At the outset of these experiments, it became apparent that twice-extracted doublets retained a relatively high orthophosphate concentration (4·8 mM mg^{-1} protein), which at pH 7·4 exists predominantly as free $H_2PO_4^-$. The concentration of P_i was linear with respect to [2×] and constant with

Table 1. *Kinetic properties of the soluble (microtubule-free) forms of the 13 S and 21 S dynein ATPases*

Preparation	V_{max} (μmol $P_i\,mg^{-1}\,min^{-1}$)	K_m (μM-ATP)	h
13 S dynein	0·97 ± 0·02 [0·4–1·7]	37 ± 3 [13–53]	1·0 ± 0·1 [0·8–1·2]
21 S dynein	0·73 ± 0·02 [0·3–0·9]	21 ± 2 [15–27]	1·0 ± 0·0 [0·9–1·1]
2× doublets	0·15 ± 0·02 [0·1–0·3]	107 ± 9 [64–112]	0·8 ± 0·1 [0·6–1·4]

All kinetic constants (V_{max}, K_m, h) were estimated by successive iteration using a non-linear least squares computer program. For 13 S and 21 S dynein, values for V_{max} and K_m were derived by eqn (1), while values for h were derived by eqn (2). All values for 2× doublets were derived by eqn (2). All values are the mean values obtained from 10 preparations of cilia. The values for standard error (±) relate to the fit of the observed dependent variables illustrated in Fig. 1. The values in brackets are the actual range of values [low–high] observed within the 10 preparations.

respect to both time and temperature and, thus, was treated as simple background. The source of P_i is unknown, but inasmuch as all processing solutions were free of phosphate, it must be native to the cilium, resulting perhaps from protein phosphatase activity and existing in a form only weakly associated with the axoneme. Although P_i is known to be a weak competitive inhibitor of dynein ATPase that reduces effective [$MgATP^{2-}$] by competing with ATP^{4-} for free Mg^{2+} (Okuno & Brokaw, 1979), its potential effect on our system is negligible because free Mg^{2+} was maintained 5 mM in excess of [ATP^{4-}), wherein [$MgATP^{2-}$] = 83 % and [Mg_2ATP] = 15 % of [ATP^{4-}] (Storer & Cornish-Bowden, 1976), and K_d for $MgATP^{2-}$ (1×10^{-4} M) is about two orders of magnitude lower than K_d for $MgHPO_4$ ($1{\cdot}3\times10^{-2}$ M). Moreover, it is evident empirically from the linear relationship of activity *versus* [2×] at saturating [ATP] that P_i is not acting as an inhibitor of residual dynein ATPase. Likewise, and although there is no evidence that microtubule-associated guanine nucleotides are accessible to the dynein ATPases, these data also eliminate the possibility that GTP or GDP may affect enzyme activity, inasmuch as they are also known to be weak competitive inhibitors of dynein ATPase (Gibbons & Gibbons, 1972).

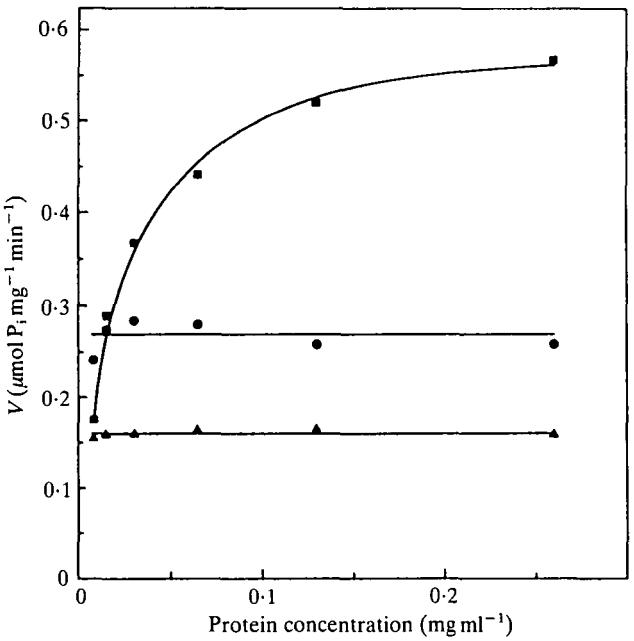

Fig. 2. Enzyme velocity plotted as specific activity (μmol P_i mg^{-1} min^{-1}) *versus* protein concentration at saturating (1 mM) concentrations of ATP. Both 21 S dynein (●) and twice-extracted doublets (▲) exhibit constant activity with respect to [protein]. However, the activity of 13 S dynein (■) increases as a saturable function of [protein], consistent with the presence of an endogenous activator in the enzyme preparation. At infinite [13 S], the specific activity of 13 S dynein was 0·59 μmol P_i mg^{-1} min^{-1} (see Table 1). Each curve was corrected for background P_i. The curve for 13 S dynein was fitted to the estimated dependent variables derived by eqn (1), but substituting *V versus* [13 S]. n = three preparations of cilia.

The specific activity of serially diluted, soluble dynein (μmol P_i mg^{-1} min^{-1}) was also examined relative to enzyme concentration and saturating and subsaturating concentrations of ATP. Like 2× doublets, both 21 S and 13 S dynein retained substantial background concentrations of P_i (1·6 and 1·3 mM mg^{-1} protein, respectively). 21 S dynein also exhibited a strict linear relationship (constant specific activity) between *V versus* [21 S] at both saturating (1 mM) and subsaturating (10 μM) concentrations of ATP (Fig. 2). However, in contrast to 21 S dynein, the specific activity of 13 S dynein increased as a saturable function of [13 S] at both saturating (1 mM) and subsaturating (30 μM) concentrations of ATP (Fig. 2), consistent with the presence of an endogenous activator in the enzyme preparation. Using equation (1) but substituting *V versus* [13 S], maximum specific activity at infinite [13 S] was 0·59 μmol P_i mg^{-1} min^{-1}, which is in the range of values obtained for the activity of soluble 13 S dynein stored at high concentration (Table 1). These values are considerably greater than the activity present at low [13 S] when the concentration was obtained by serial dilution (0·16 μmol P_i mg^{-1} min^{-1}). The concentration-dependent behaviour of 13 S dynein probably accounts for the greater variability encountered in the estimated kinetic parameters for soluble 13 S dynein (Table 1), inasmuch as activity was generally measured relative to small volumes of enzyme removed from concentrated stock solutions.

Kinetic properties of the microtubule-activated dyneins

Previously we reported that when soluble 13 S or 21 S dynein was mixed with twice-extracted doublets, the resulting ATPase activity was stimulated several-fold and was accompanied by restoration of inner row or outer row dynein arms (Warner *et al.* 1985). To characterize dynein activation by microtubules, 13 S or 21 S dynein (8 μg ml^{-1}) was mixed with increasing concentrations of 2× doublets (0·03–0·51 mg ml^{-1}) and ATPase activity was determined under standard assay conditions (1 mM-ATP). The activity of 2× doublets alone (nmol P_i ml^{-1} min^{-1}), within the limits of assay sensitivity, was linear at protein concentrations $<0{\cdot}3$ mg ml^{-1} but became decidedly non-linear at concentrations $>0{\cdot}3$ mg ml^{-1} (Fig. 3). As a consequence, ATPase activity of the 13 S + 2× or 21 S + 2× mixtures also exhibited non-linear behaviour at high protein concentrations (Fig. 3), although total ATPase activity was clearly greater than the activity contributed by the 2× doublets or soluble dyneins alone. At present we have no explanation for the non-linear behaviour, although it may relate to substrate depletion owing to ineffectiveness of the ATP-regenerating system when used in combination with extracted doublets. Non-linearity could limit the accuracy of our kinetic assays done at high protein concentrations; however, most of our data were derived at low protein concentrations ($<0{\cdot}3$ mg ml^{-1}) where ATPase activity was linear (see below). After subtracting residual ATPase activity of the 2× doublets from the mixed preparations, the remaining activity associated with both dyneins (μmol P_i mg^{-1} min^{-1}) appeared to exhibit simple saturation behaviour with respect to [2×]. For 21 S dynein, velocity at [2×] = 0·51 mg ml^{-1} was >60 % of V_{max} estimated by equation (1) and, thus, a doublet concentration $\leqq 0{\cdot}51$ mg ml^{-1} was sufficient to derive kinetic parameters

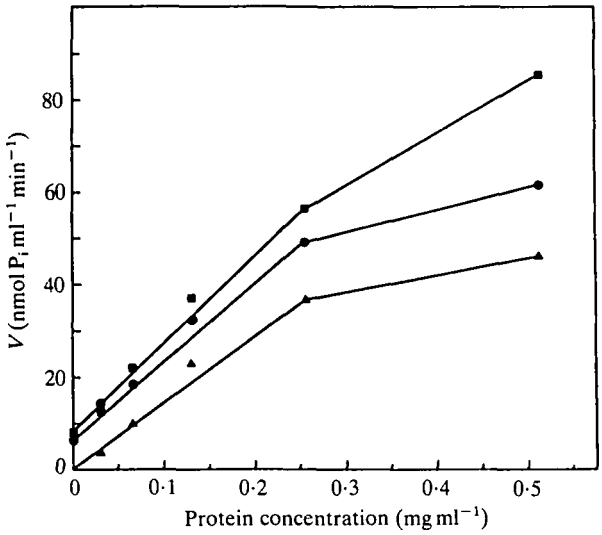

Fig. 3. Total ATPase activity (nmol P_i ml^{-1} min^{-1}) for variable concentrations of twice-extracted doublets (▲), and 2× doublets mixed with 13 S (■) or 21 S (●) dynein (8 $\mu g\,ml^{-1}$). For these preparations, the basal activity of the soluble dyneins was 6–8 nmol P_i ml^{-1} min^{-1}. n = two preparations of cilia.

for 21 S dynein. However, for 13 S dynein, velocity at [2×] = 0·51 mg ml^{-1} was only 38 % of the estimated V_{max}. Use of higher concentrations of 2× doublets ($\geqq$1 mg ml^{-1}) was ineffective because the residual activity of the doublets introduced an unfavourable signal-to-noise ratio into the data, restricting the extent of our kinetic analysis of 13 S dynein (see below). For the data illustrated in Fig. 3, 13 S dynein was activated fivefold and 21 S dynein was activated 2·5-fold at [2×] = 0·51 mg ml^{-1} and 1 mM-ATP.

In order to determine true kinetic parameters for the microtubule-activated dyneins at infinite [2×] and [ATP], substrate saturation kinetics were determined relative to five concentrations of activating 2× protein obtained by serial dilution (0·032, 0·06, 0·13, 0·26 and 0·51 mg ml^{-1}; dynein = 8 $\mu g\,ml^{-1}$). To maintain internal consistency in these experiments, saturation kinetics for 13 S dynein, 21 S dynein, 2× doublets, 13 S + 2× doublets and 21 S + 2× doublets were done simultaneously from the same preparations of cilia. The dependent variables (V) obtained from each of two preparations were averaged and the mean values analysed by equations (1) or (2). For all experiments using equation (2), curves were fitted using four to eight data points (2–4 points at [ATP] < $[S]_{0.5}$).

Because at high protein concentrations residual ATPase activity of the doublets can constitute a significant proportion of total activity (2× + 13 S or 2× + 21 S) and thus interfere with analysis of dynein-related activity, we used [2×] $\leqq$ 0·51 mg ml^{-1} which, as noted above, was sufficient for a complete kinetic analysis of 21 S dynein but insufficient for 13 S dynein. For the following experiments, the relative proportions of ATPase activity contributed to total activity by the added dyneins are summarized in Table 2. At the protein concentrations used, added dynein contributed a maximum of 75 % and a minimum of 25 % to total activity.

Although the kinetic analysis that follows depends on subtracting residual ATPase activity of the 2× doublets from total activity to derive kinetic parameters for the microtubule-activated dyneins, we also analysed kinetic parameters relative to total ATPase activity of the combined preparations. For example, as illustrated in Fig. 4, both the 13 S and 21 S dyneins (8 μg ml^{-1}) when mixed with 2× doublets (0·064 mg ml^{-1}) exhibit sigmoid saturation kinetics ($h \cong 1{\cdot}4$), in contrast to the simple saturation kinetics ($h = 1{\cdot}0$) associated with the 2× doublets or soluble dyneins alone. Moreover, both the Hill coefficient and the Michaelis constant derived for total activity uniformly exceeded the range of values observed for the soluble dyneins (Table 1). This behaviour held for every preparation of axonemes examined and for each concentration of 2× protein used to activate the dyneins.

The results from a typical kinetic experiment done at [2×] = 0·26 mg ml^{-1} (after subtracting residual activity) are illustrated in Figs 5 (13 S) and 6 (21 S). Both 13 S and 21 S dynein in the presence of microtubules exhibit a significant shift to sigmoid saturation kinetics ($h \geqq 2{\cdot}0$) accompanied by a considerable increase in both V_{max} and K_m ($[S]_{0{\cdot}5}$). For purposes of estimating kinetic behaviour, we must first distinguish between true enzyme velocity (V) and apparent velocity (V_{app}) because use of equations (1) or (2) relative to [2×] requires that the enzymes have no activity in the absence of extracted doublets. Because the microtubule-free dyneins have significant basal activity, this activity was subtracted from observed velocity at each [2×] to yield V_{app} and then re-added to yield true V_{max} (Table 3). In order to estimate the kinetic parameters at infinite [2×] and [ATP], values for V_{max} at infinite [ATP] and each of four concentrations of 2× doublets were obtained (Table 3) and then analysed by equation (1) (V_{max} *versus* [2×]; Fig. 7). For 21 S dynein, infinite [2×] and [ATP] yield $V_{max} = 2{\cdot}65$ μmol P_i mg^{-1} min^{-1}, with an apparent $K_d = 0{\cdot}51$ mg ml^{-1} (see below). Owing to the limitation on 13 S kinetics discussed earlier, we can at present carry the analysis of 13 S dynein no further than the data summarized in Table 3. However, by equation (1), $V_{max} = 9{\cdot}54$ μmol P_i mg^{-1} min^{-1}, although the range of values observed in different experiments on 13 S dynein was very large (4–16 μmol P_i mg^{-1} min^{-1}).

Table 2. *Sources of ATPase activity for the microtubule-activated dyneins*

[2×] (mg ml^{-1})	2× (nmol P_i ml^{-1} min^{-1})	2×+13 S (nmol P_i ml^{-1} min^{-1})	(%)	2×+21 S (nmol P_i ml^{-1} min^{-1})	(%)
0·032	3·5	12·5	72	14·3	75
0·064	10·2	21·8	53	18·6	45
0·128	23·0	37·1	38	32·0	28
0·256	35·8	56·3	36	48·6	26
0·512	46·1	85·5	46	61·4	25

Total ATPase activity for variable concentrations of twice-extracted doublets [2×] and 2× doublets to which have been added 13 S or 21 S dynein (8 μg ml^{-1}). All values are the mean values from the two experiments used to derive Figs 7–9 and are expressed as nmol P_i ml^{-1} min^{-1} in 1 mM-ATP. Values for the 2×+13 S or 2×+21 S preparations are also expressed as the % of total activity contributed by added dynein (total activity minus activity of the 2× doublets).

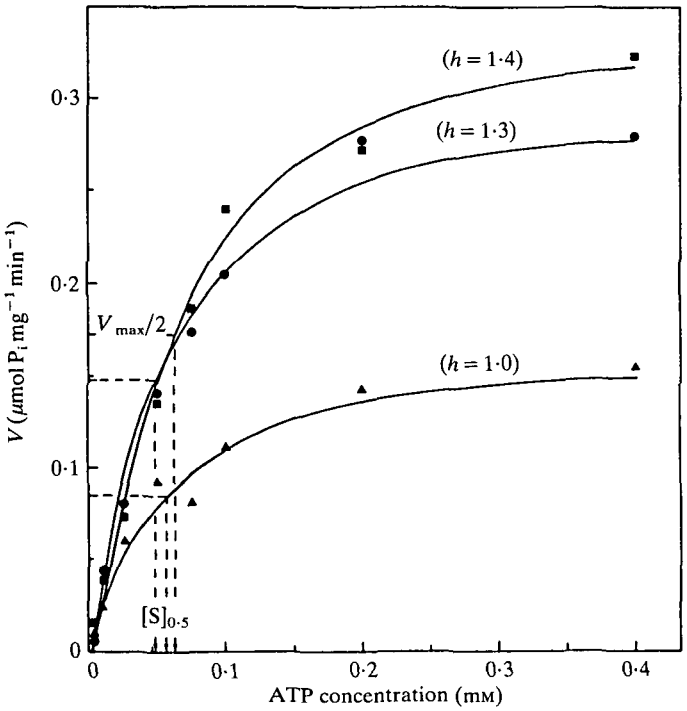

Fig. 4. Total ATPase activity (μmol P_i mg protein^{-1} min^{-1}) for 2× doublets (▲; 0·064 mg ml^{-1}) and 2× doublets mixed with 13 S (■) or 21 S (●) dynein (8 μg ml^{-1}). The curves were fitted to the estimated dependent variables derived by eqn (2). Both enzymes in the presence of 2× protein exhibit sigmoid saturation kinetics (h = 1·3–1·4), while 2× doublets (or dynein) alone exhibit simple saturation kinetics (h = 1·0). n = one preparation of cilia.

However, for 21 S dynein, values for all three kinetic parameters (V_{max}, $[S]_{0.5}$ and h) at infinite [ATP] and [2×] can be derived by replotting velocity (V) from the data used to derive the parameters in Table 3 but at four concentrations of ATP (0·1, 0·2, 0·4, 1·0 mM) *versus* three concentrations of doublets (0·06, 0·13, 0·51 mg ml^{-1}) (Fig. 8). Equation (1) then yields V_{max} at infinite [2×] for each given [ATP], and if V_{max} obtained for each [ATP] (Fig. 8) is then plotted *versus* [ATP] (Fig. 9), we obtain by equation (2) estimates of true V_{max}, $[S]_{0.5}$ and h. For 21 S dynein, V_{max} = 2·62 μmol P_i mg^{-1} min^{-1}, $[S]_{0.5}$ = 141 μM-ATP and $h \approx 1.9$. In principle, V_{max} obtained by equation (2) (Fig. 9; V_{max} *versus* [ATP]) should agree, as it does, with the value obtained by equation (1) (Fig. 7; V_{max} *versus* [2×]). The average velocity for 21 S dynein (2·64 μmol P_i mg^{-1} min^{-1}) converts to a turnover rate of 88 mol ATP per mol E s^{-1} (M_r 21 S = 2×10^6; Johnson & Wall, 1983). The tentative velocity for 13 S dynein (9·54 μmol P_i mg^{-1} min^{-1}) yields a turnover rate of 95 mol ATP per mol E s^{-1} (M_r 13 S = 6×10^5; Gibbons & Rowe, 1965). Although the pattern of changes occurring in the kinetic parameters of the activated dyneins is consistent relative to increasing concentrations of activating protein (Table 3), because of the non-linear ATPase activity discussed earlier (Fig. 3) we urge caution

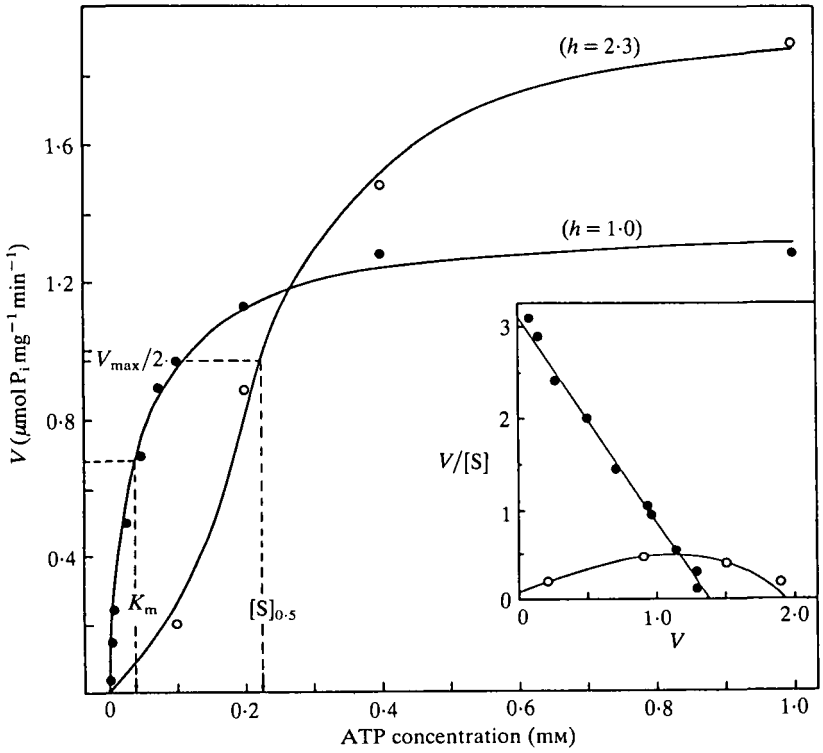

Fig. 5. Substrate (ATP) saturation kinetics (direct plot) for soluble 13 S dynein (●) and 13 S dynein activated with 0·26 mg ml^{-1} 2× doublets (○). The curves were fitted to the estimated dependent variables derived by eqn (1) or (2). Microtubule-activated 13 S dynein exhibits an increase in velocity, a decrease in the Michaelis constant ($[S]_{0.5}$), and a shift to sigmoid saturation kinetics ($h = 2{\cdot}3$). The insert is an Eadie–Scatchard plot of the same data. n = three preparations of cilia.

when interpreting values for the three parameters since they may be slight underestimates of the true values.

In principle, an approximate dissociation constant (K_d) for the dynein–microtubule complex can also be determined from data illustrated in Fig. 8. However, because we do not know the identity of the activating ligand (presumably tubulin), the parameter is meaningful only in view of the changes that it undergoes as a result of dynein activation or ligand binding. Just as activation of 21 S dynein results in a systematic increase in $[S]_{0.5}$ (Table 3), activation also results in a systematic increase in apparent K_d. Using equation (2) but substituting K_d *versus* [ATP] (from Fig. 8), $K_d = 0{\cdot}42$ mg ml^{-1} at infinite [ATP] and [2×].

DISCUSSION

By permitting the soluble forms of the 13 S and 21 S dynein ATPases to react with extracted doublet microtubules under conditions that restore inner row and outer row dynein arms (Warner *et al.* 1985), we have shown that rebinding of dynein to the microtubule lattice activates ATPase activity to a turnover rate of about 90 mol ATP

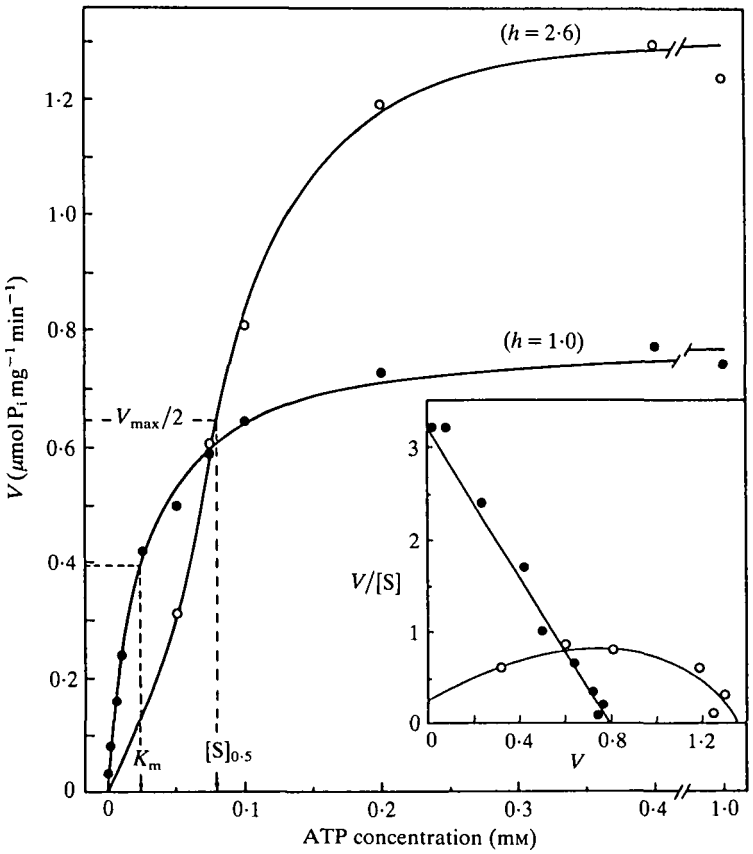

Fig. 6. Substrate (ATP) saturation kinetics (direct plot) for soluble 21 S dynein (●) and 21 S dynein activated with 0·26 mg ml^{-1} 2× doublets (○). The curves were fitted to the estimated dependent variables derived by eqn (1) or (2). Microtubule-activated 21 S dynein exhibits an increase in velocity, a decrease in the Michaelis constant ($[S]_{0.5}$) and a shift to sigmoid saturation kinetics ($h = 2{\cdot}6$). The insert is an Eadie–Scatchard plot of the same data. n = three preparations of cilia.

per mol E s^{-1} and at the same time decreases the affinity of the two enzymes for $MgATP^{2-}$ and microtubules. These characteristics are accompanied by a shift from hyperbolic saturation kinetics ($h = 1{\cdot}0$) to sigmoid kinetics ($h = 2$–3). It may be inferred that these properties approximate physiological behaviour for the functional or microtubule-activated conformations of the two dynein ATPases.

The soluble dyneins from a variety of organisms have always exhibited considerable activity in their microtubule-free conformations, regardless of the organism or method by which they were isolated, although this basal activity has been termed latent because it can be increased or activated by several different methods (Gibbons & Fronk, 1979). Basal activity typically exhibits simple saturation kinetics ($h = 1{\cdot}0$) and spans a rather broad range of values (0·2–3 μmol P_i mg^{-1} min^{-1}), although anti-sigmoid kinetics have been reported for soluble *Tetrahymena* 21 S dynein (Shimizu, 1981). The Michaelis constant (K_m) likewise exhibits a considerable range (10–50 μM-ATP), although higher affinity sites (≅1 μM-ATP) have been reported

(Johnson, 1983; Shimizu, 1981). In the case of 13 S dynein, basal activity is related in part to the presence of a co-purifying, activating ligand (Fig. 2). However, the conformation of the soluble dynein particle may also have a considerable effect on its activity inasmuch as it can be quite different from the highly ordered, overlapping

Table 3. *Microtubule-induced activation of the 13 S and 21 S dynein ATPases*

Preparation	[2×] (mg ml^{-1})	V_{max} (μmol P_i mg^{-1} min^{-1})	V_{app} (μmol P_i mg^{-1} min^{-1})	$[S]_{0.5}$ (μM-ATP)	h
13 S dynein	0	1·01 ± 0·02	—	35 ± 3	1·0
	0·032	1·14 ± 0·04	0·12	39 ± 3	2·2 ± 0·3
	0·064	1·24 ± 0·03	0·23	62 ± 1	2·0 ± 0·1
	0·128	1·69 ± 0·01	0·68	75 ± 1	1·7 ± 0·1
	0·256	2·52 ± 0·01	1·50	127 ± 6	1·9 ± 0·1
21 S dynein	0	0·77 ± 0·02	—	26 ± 2	1·0
	0·064	1·02 ± 0·01	0·24	49 ± 2	1·7 ± 0·1
	0·128	1·09 ± 0·03	0·31	62 ± 5	1·5 ± 0·1
	0·256	1·45 ± 0·05	0·68	82 ± 4	3·2 ± 0·5
	0·512	1·70 ± 0·01	0·93	96 ± 8	3·7 ± 1·2

Values for enzyme velocity (V_{max}, V_{app}) at different microtubule concentrations [2×] were derived by eqn (2) after correcting for residual activity of the 2× doublets. Values for velocity at $[2\times]_0$ were derived by eqn (1). The values for standard error (±) relate to the fit of the observed dependent variables as in Figs 5 and 6. All values are the mean values obtained from two preparations of cilia.

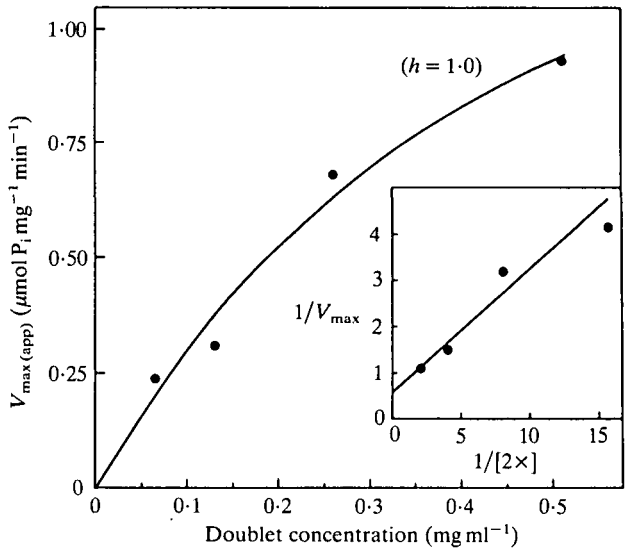

Fig. 7. Direct plot of apparent maximum velocity of 21 S dynein at four concentrations of 2× doublets (0·06–0·51 mg ml^{-1}). The data were taken from the experiments summarized in Table 3 and fitted to the estimated dependent variables derived by eqn (1) (V_{max} = 2·65 μmol P_i mg^{-1} min^{-1}). The insert is a Lineweaver–Burke plot of the same data. n = two preparations of cilia.

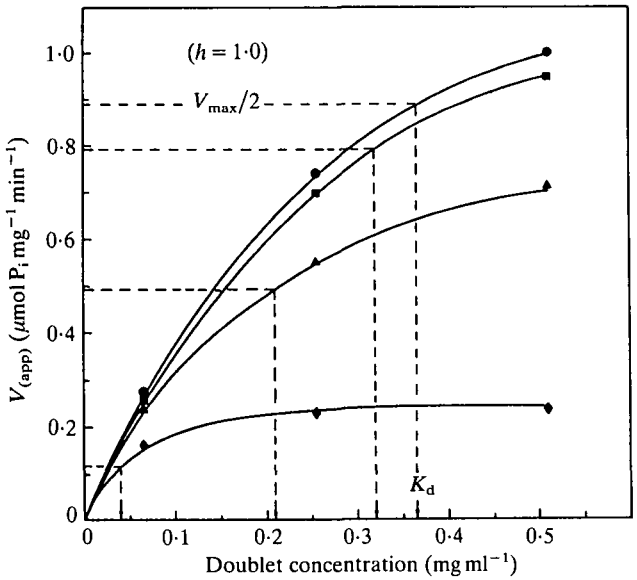

Fig. 8. Direct plot of apparent velocity of 21 S dynein *versus* [2×] at four concentrations of ATP (0·1–1 mM). The data were taken from the experiments summarized in Table 3 and fitted to the estimated dependent variables derived by eqn (1). The apparent dissociation constant (K_d) increases as a function of increasing [ATP] to a maximum value of 0·42 mg ml^{-1} at infinite [2×] and [ATP]. Values for V_{max} derived at each ATP concentration are plotted in Fig. 9. (●) 1·0 mM; (■) 0·4 mM; (▲) 0·2 mM; (◆) 0·1 mM-ATP.

array of outer row dynein arms found in native cilia or flagella (Goodenough & Heuser, 1984). The potential effect of conformation on activity is particularly evident when comparing the turnover rates for the soluble forms of the two enzymes. Even though it is partially activated, the basal turnover rate for 13 S dynein (10 mol ATP per mol E s^{-1}) is considerably lower than the basal rate for 21 S dynein (24 mol ATP per mol E s^{-1}).

Under our experimental conditions, the kinetic behaviour of soluble 13 S and 21 S dynein from *Tetrahymena*, with minor exceptions, was not significantly different from behaviour reported previously (Gibbons, 1966). However, saturation kinetics for the activated forms of the dynein ATPases have not been described previously. Because extracted doublet microtubules retain many of their accessory proteins and structures when they are used to activate the soluble dyneins, we cannot be certain that activation is derived solely from the effect of a single ligand or even from the same ligand for both dyneins. However, using microtubules reassembled from highly purified brain tubulin, Omoto & Johnson (1984) have shown that 21 S dynein is activated by polymeric tubulin. In our experiments, the most significant activation-related change in behaviour occurs in the form of sigmoid saturation kinetics. Although sigmoid kinetics can be generated by other properties of an enzyme, in a rapid equilibrium system they are most frequently related to positive cooperativity, particularly if binding of the activating ligand by the enzyme also exhibits sigmoid kinetics. Although saturation of the doublet microtubule lattice with exogenous 21 S

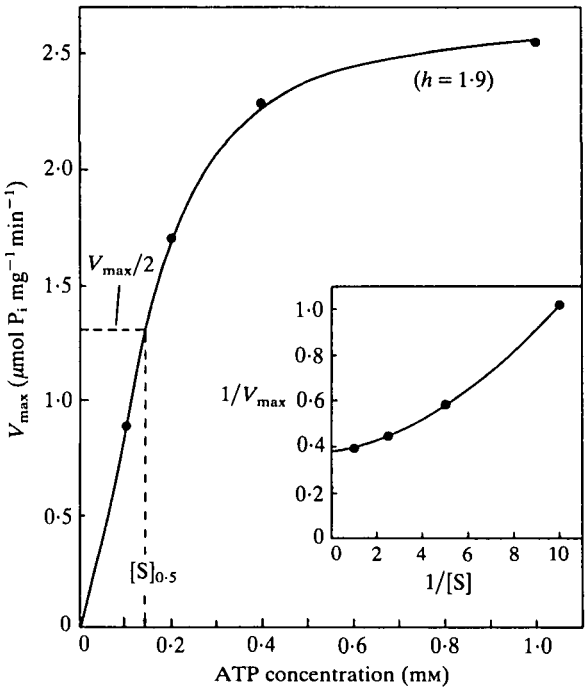

Fig. 9. Direct plot of V_{max} for 21 S dynein derived at four ATP concentrations (see legend to Fig. 8) *versus* [ATP]. The data are fitted to the estimated dependent variables derived by eqn (2) and yield V_{max} (2·62 μmol P_i mg^{-1} min^{-1}), $[S]_{0.5}$ (141 μM-ATP) and h (1·9) at infinite [ATP] and [2×]. The insert is a Lineweaver–Burke plot of the same data.

dynein exhibits strong sigmoid behaviour ($h = 4.5$; Db *versus* Df, derived from Warner & McIlvain, 1982), as noted, it is unlikely that this behaviour is related to true allosteric interactions between tubulin-binding domains on the dynein particle.

The Hill coefficient for activated 13 S dynein was uniformly determined to be ≅2·0 (Table 3), consistent with positive cooperativity between a minimum of two interacting sites and the presence of two ATPase subunits in the inner arm particle (Piperno & Luck, 1981). In contrast, the Hill coefficient for 21 S dynein exhibited a broader range of values and frequently was ⩾3·0 (Table 3), consistent with a minimum of three interacting sites and the presence of three ATPase subunits in the outer arm particle (Johnson, 1983). Although for the experiments summarized in Fig. 9, h derived for 21 S dynein at infinite [ATP] and [2×] was only 1·9, this lower value may simply reflect insufficient data at ATP concentrations $<[S]_{0.5}$.

The behaviour of the two dynein ATPases may have important implications for understanding how dynein activity is coupled to motility. If this apparent co-operativity is occurring relative to a minimum to two (13 S) and possibly three (21 S) interacting sites, it seems likely to be related to subunit interactions within individual dynein particles. However, in the case of the dynein ATPases, the practical definition of cooperativity may have to be extended to include not only allosteric interactions between subunits of the 13 S or 21 S particles, but also the possibility of

specific interactions between subunits of adjacent dynein arms. If we postulate that a row of dynein arms is analogous to an enzyme oligomer, interactions between subunits (arms) of the oligomer may then be true allosteric interactions. The practical consequences of such behaviour could be to provide a (necessary) mechanism for regulating dynein activity at the leading and, or, trailing edges of a propagating bend. The absence of detectable cooperativity in the ATPase activity of the soluble forms of the two dyneins may be related to the absence of conformational stability that otherwise exists with dynein arms *in situ*, although interaction with an activating ligand may also be required for integrated activity of the different ATPase domains. It is worth noting that soluble 13 S dynein, even though partially activated by a copurifying ligand (Fig. 2), nonetheless exhibits simple saturation kinetics only (Table 1). Sigmoid kinetics occur only after addition of microtubules (Table 3).

The maximum velocity of activated 21 S dynein was stimulated about fourfold at infinite [ATP] and [2×] and was accompanied by a considerable decrease in both substrate and microtubule affinity. Although we were unable to determine kinetic parameters for 13 S dynein at infinite [ATP] and [2×], the kinetic behaviour of activated 13 S dynein appeared to be very similar to that of 21 S dynein (Table 3). Although based on qualitatively similar enzymic mechanisms (Johnson, 1983), the steady-state behaviour of the dynein ATPases is in part very different from that of actin-activated myosin ATPase. Even allowing for variability resulting from different experimental conditions, actin-activated heavy meromyosin exhibits no apparent cooperativity and has a maximum turnover rate of about 30 mol ATP per mol E s^{-1} (M_r $4{\cdot}7\times10^5$) and a correspondingly lower K_m (6 μM-ATP) (Eisenberg & Moos, 1970). The rate of product release determines the steady-state turnover rate for both myosin and dynein, and the rate for soluble dynein is about 100-fold faster than the rate for soluble myosin (Johnson, 1983). On the basis of the considerable difference in the Michaelis constant for the soluble and activated forms of dynein, product release by activated dynein is likely to be even faster. $[S]_{0.5}$ for activated 21 S dynein (141 μM-ATP) may underestimate the true value owing to limited data at ATP concentrations $<[S]_{0.5}$ (Fig. 9); however, it is consistent with the K_m determined for motility-coupled ATPase activity in reactivated sea-urchin sperm flagella ($\geqslant$100 μM-ATP; Gibbons & Gibbons, 1972). In contrast to microtubule-activated dynein, motility-coupled dynein activity, expressed either as beat frequency or enzyme velocity, has generally exhibited hyperbolic to anti-sigmoid saturation kinetics (Gibbons & Gibbons, 1972; Okuno & Brokaw, 1979). However, apparent saturation kinetics for motility-coupled activity may result from the normal superimposition of several interacting mechanisms or regulatory events rather than resulting solely from the kinetic behaviour of one or both dyneins.

The capability of evaluating independently the kinetic behaviour of the two dynein ATPases when recombined with native microtubules should provide an important means for studying motility-coupled ATPase activity as a function of the two rows of dynein arms.

This study was supported by research grant GM20690 from the National Institutes of Health.

REFERENCES

BRADFORD, M. M. (1976). A rapid and sensitive method for the quantitation of microgram quantities of protein utilizing the principle of protein dye-binding. *Analyt. Biochem.* **72**, 248–254.

EISENBERG, E. & MOOS, C. (1970). Actin activation of heavy meromyosin adenosine triphosphatase. *J. biol. Chem.* **245**, 2451–2456.

GIBBONS, B. H. & GIBBONS, I. R. (1972). Flagellar movement and adenosine triphosphatase activity in sea urchin sperm extracted with Triton X-100. *J. Cell Biol.* **54**, 75–97.

GIBBONS, I. R. (1966). Studies on the adenosine triphosphatase activity of 14 S and 30 S dynein from cilia of *Tetrahymena*. *J. biol. Chem.* **241**, 5590–5596.

GIBBONS, I. R. & FRONK, E. (1979). A latent adenosine triphosphatase form of dynein 1 from sea urchin. *J. biol. Chem.* **254**, 187–196.

GIBBONS, I. R. & ROWE, A. J. (1965). Dynein: a protein with adenosine triphosphatase activity from cilia. *Science* **149**, 424–426.

GOODENOUGH, U. W. & HEUSER, J. E. (1984). Structural comparison of purified dynein proteins with *in situ* dynein arms. *J. molec. Biol.* **180**, 1083–1118.

GOODENOUGH, U. W. & HEUSER, J. E. (1985). Structure of inner dynein arms, radial spokes, and the central pair/projection complex of cilia and flagella. *J. Cell Biol.* **100**, 2008–2018.

JOHNSON, K. A. (1983). The pathway of ATP hydrolysis by dynein. Kinetics of a presteady state phosphate burst. *J. biol. Chem.* **258**, 13 825–13 832.

JOHNSON, K. A. & WALL, J. S. (1983). Structure and molecular weight of the dynein ATPase. *J. Cell Biol.* **96**, 669–678.

MITCHELL, D. R. & WARNER, F. D. (1980). Interactions of dynein arms with B subfibers of *Tetrahymena* cilia. Quantitation of the effects of magnesium and adenosine triphosphate. *J. Cell Biol.* **87**, 84–97.

MITCHELL, D. R. & WARNER, F. D. (1981). Binding of dynein 21 S ATPase to microtubules. Effects of ionic conditions and substrate analogs. *J. biol. Chem.* **256**, 12 535–12 544.

OKUNO, M. & BROKAW, C. J. (1979). Inhibition of movement of Triton-demembranated sea urchin sperm flagella by Mg^{2+}, ATP^{4-}, ADP and P_i. *J. Cell Sci.* **38**, 105–123.

OMOTO, C. K. & JOHNSON, K. A. (1984). Activation of dynein ATPase by microtubules. *J. Cell Biol.* **99**, 350a (abstr.).

PIPERNO, G. & LUCK, D. J. L. (1981). Inner arm dyneins from flagella of *Chlamydomonas reinhardtii*. *Cell* **27**, 331–340.

PORTER, M. E. & JOHNSON, K. A. (1983). Characterization of the ATP-sensitive binding of *Tetrahymena* 30 S dynein to bovine brain microtubules. *J. biol. Chem.* **258**, 6575–6581.

READ, S. M. & NORTHCOTE, D. H. (1981). Minimization of variation in the response to different proteins of the Coomassie Blue G dye-binding assay for protein. *Analyt. Biochem.* **116**, 53–59.

SHIMIZU, T. (1981). Steady-state kinetic study of vanadate-induced inhibition of ciliary dynein adenosinetriphosphatase activity from *Tetrahymena*. *Biochemistry* **20**, 4347–4354.

STORER, A. C. & CORNISH-BOWDEN, A. (1976). Concentration of $MgATP^{2-}$ and other ions in solution. *Biochem. J.* **157**, 1–5.

TAUSSKY, H. H. & SHORR, E. (1953). A microcolorimetric method for the determination of inorganic phosphate. *J. biol. Chem.* **202**, 675–685.

WARNER, F. D. & MCILVAIN, J. H. (1982). Binding stoichiometry of 21 S dynein to A and B subfiber microtubules. *Cell Motil.* **2**, 429–443.

WARNER, F. D., PERREAULT, J. G. & MCILVAIN, J. H. (1985). Rebinding of *Tetrahymena* 13 S and 21 S dynein ATPases to extracted doublet microtubules. The inner row and outer row dynein arms. *J. Cell Sci.* **77**, 263–287.

(Received 12 July 1985 – Accepted, in revised form, 17 February 1986)